Supplementary Information

Rapid identification of newly emerging influenza viruses by surface-enhanced Raman spectroscopy

Jae-young Lim†[a], Jung-soo Nam†[b], Se-eun Yang†[a], Hyunku Shin[a], Yoon-ha Jang[b], Gyu-Un Bae[c], Tae-wook Kang[d], Kwang-il Lim,*[b] and Yeonho Choi,*[a,e]

[a] Department of Bio-convergence Engineering, Korea University, Seoul, 136-713, Korea

[b] Department of Medical & Pharmaceutical Sciences, Sookmyung Women's University, Seoul, 140-742, Korea

[c] Research Center for Cell Fate Control, College of Pharmacy, Sookmyung Women's University, Seoul, 140-742, Korea

[d] Department of Chemical & Biomolecular Engineering, Sogang University, Seoul, 121-742, Korea

[e] School of Biomedical Engineering, Korea University, Seoul, 136-713, Korea`

† These authors equally contributed to this work.

*To whom correspondence should be addressed.

E-mail: yeonhochoi@korea.ac.kr and klim@sookmyung.ac.kr

KEYWORDS: Influenza virus, Raman scattering, Plasmonics, Virus detection, SERS

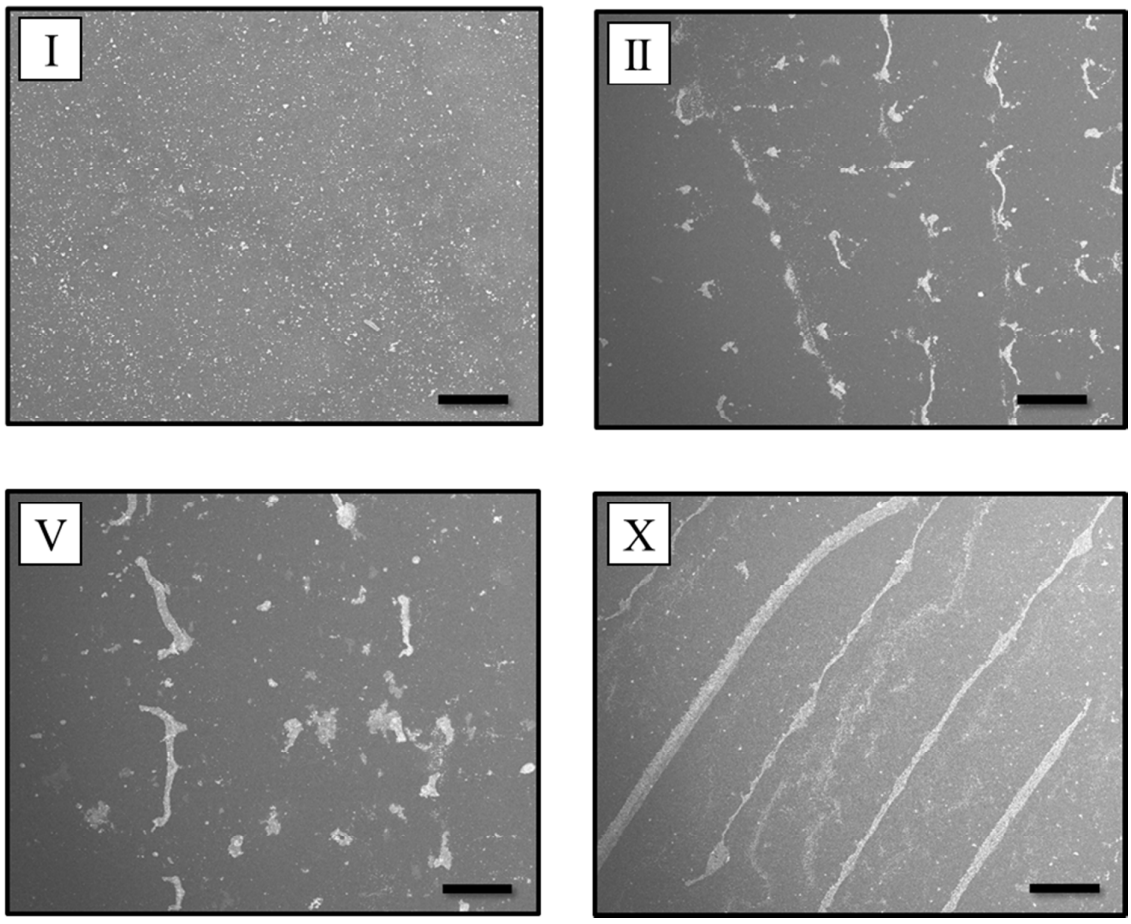

Figure S1

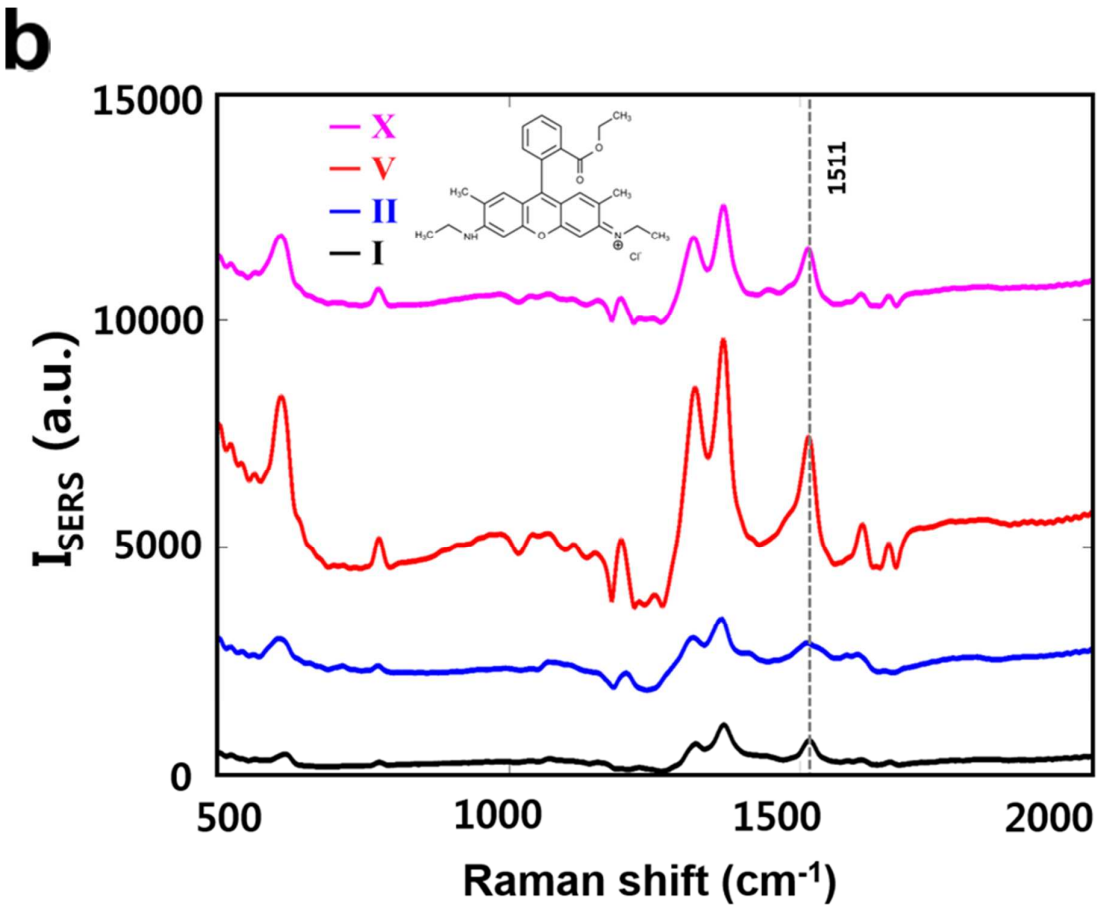
b
15000
10000
5000
0
X
V
II
I
1511
I_{SERS} (a.u.)
500
1000
1500
2000
Raman shift (cm^{-1})

Figure S1

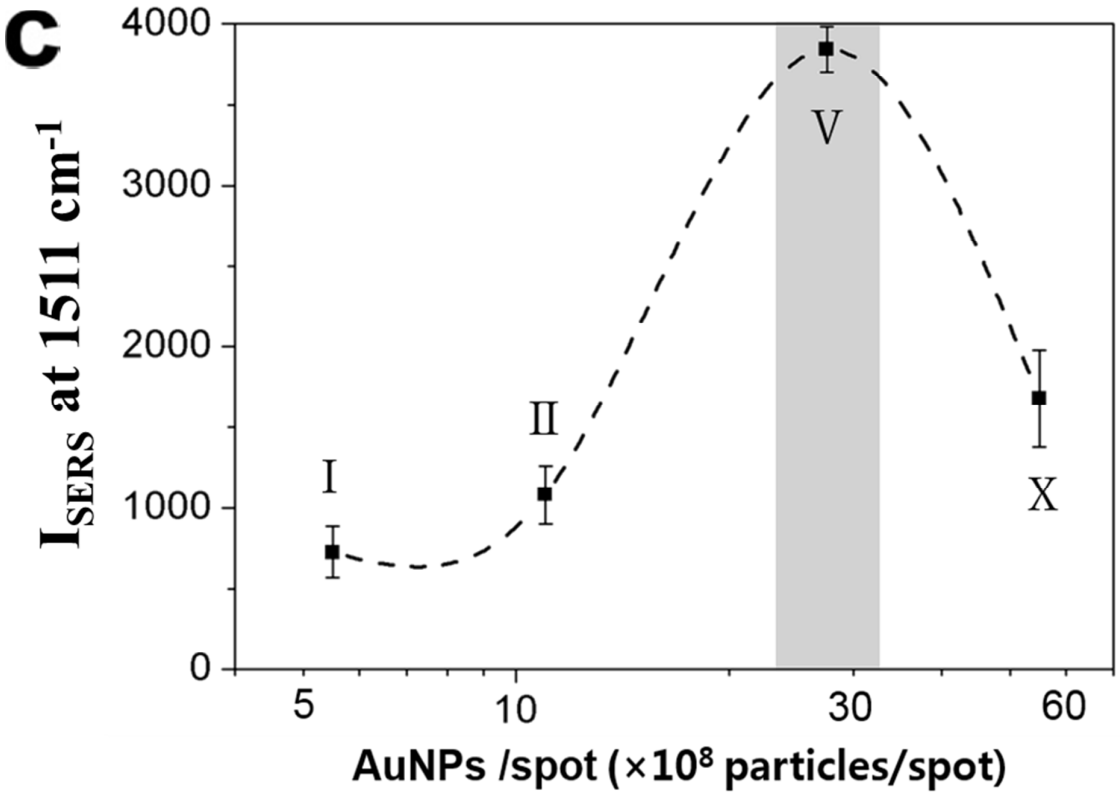

Figure S1. Characterization of SERS substrates.

(a) Representative SEM images of GNP aggregates that were prepared with different concentrations of GNP solution. The concentrations of GNP are 0.29 (I), 0.58 (II), 1.45 (V), and 2.9 mM (X), respectively. The scale bars indicate 10 μm. (b) SERS spectrum from 1 μM R6G molecules on substrates that were prepared with GNP of different concentration. (c) Changes in the intensity of R6G Raman spectra at 1511 cm^{-1} as a function of GNP concentration (ranging from 0.29 to 2.9 mM). (Spot: 19.625 mm^2 SERS active site) Spot means the area of PDMS well.

Figure S1

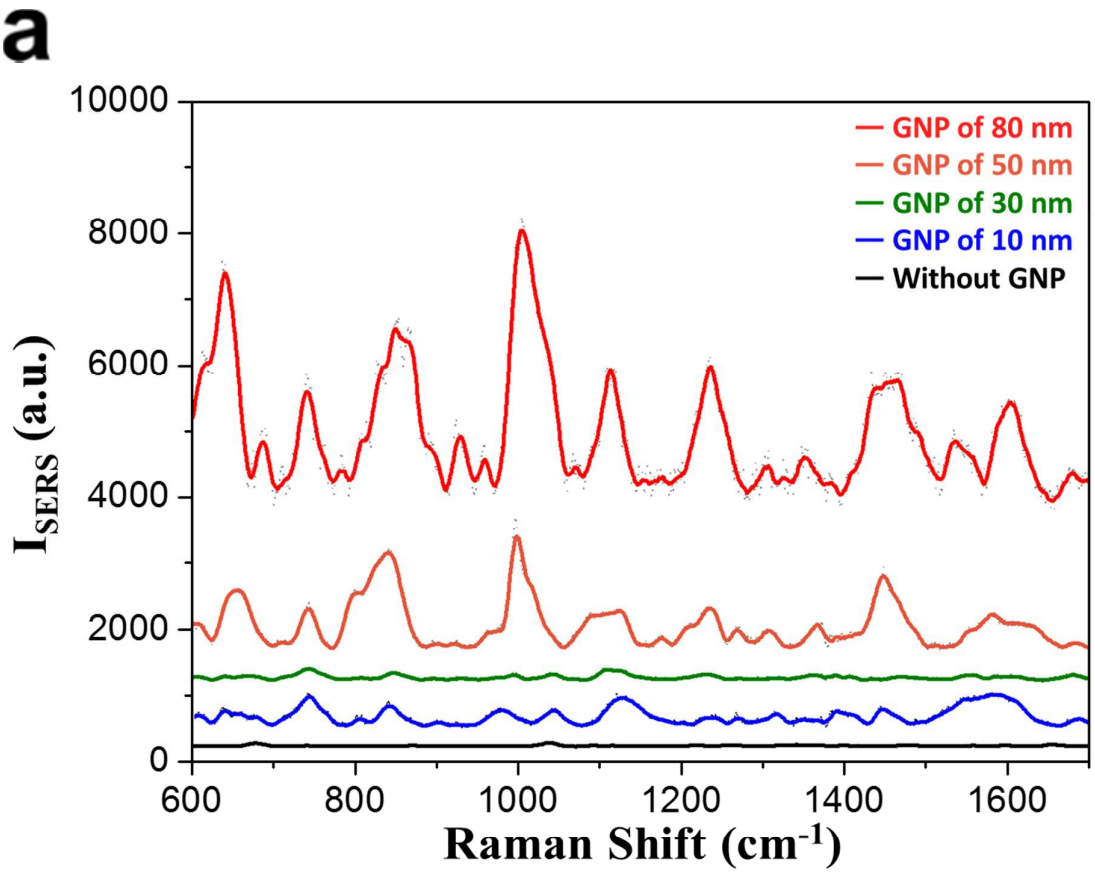
a
10000
8000
6000
4000
2000
0
600
800
1000
1200
1400
1600
I_SERS (a.u.)
Raman Shift (cm-1)
GNP of 80 nm
GNP of 50 nm
GNP of 30 nm
GNP of 10 nm
Without GNP

Figure S2

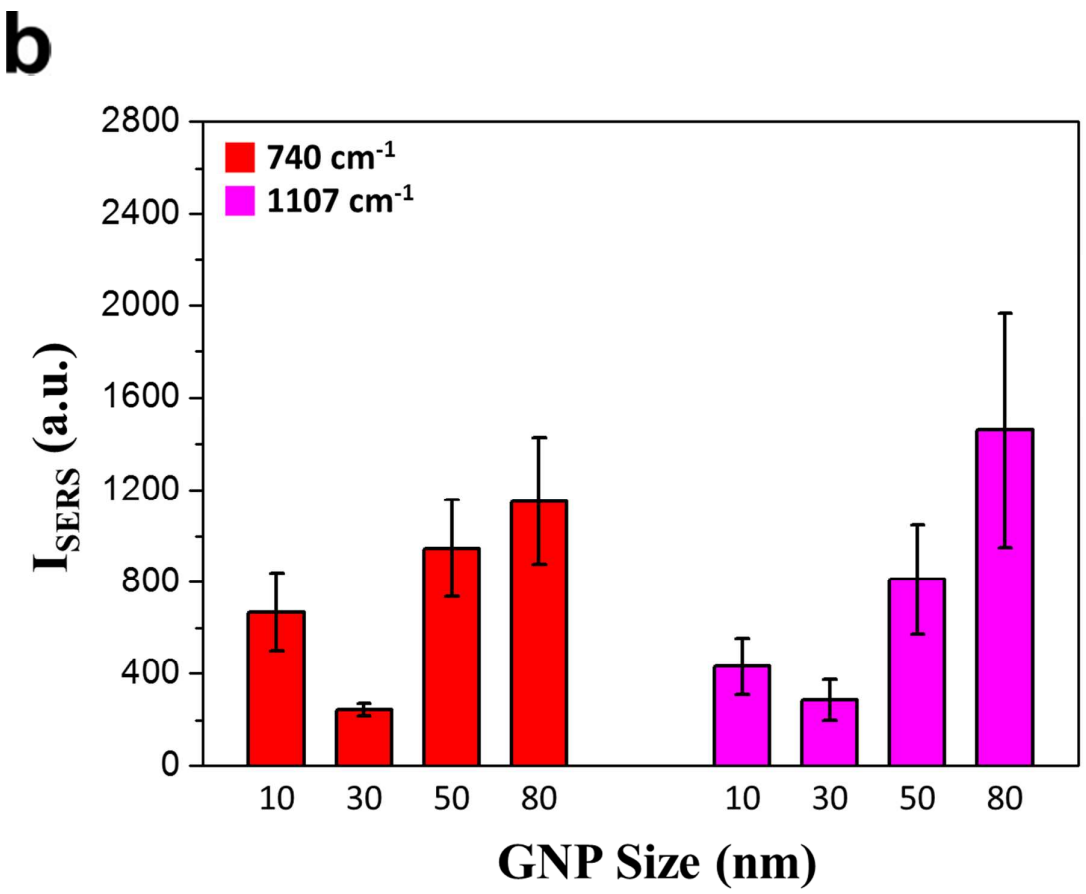

Figure S2. Optimization of GNP size for better enhancing viral SERS signal.

(a) The quality of SERS spectra highly depended on the GNP size. GNP substrates were applied at the same concentration independent of their size and aggregated at 10 mM $CuSO_4$. (b) SERS intensities measured at 740 cm^{-1}, and 1107 cm^{-1}. Each error bar corresponds to the half standard deviation of ten independent measurements. Raman signals from $V_{WSN\ HA+NA}$ were measured.

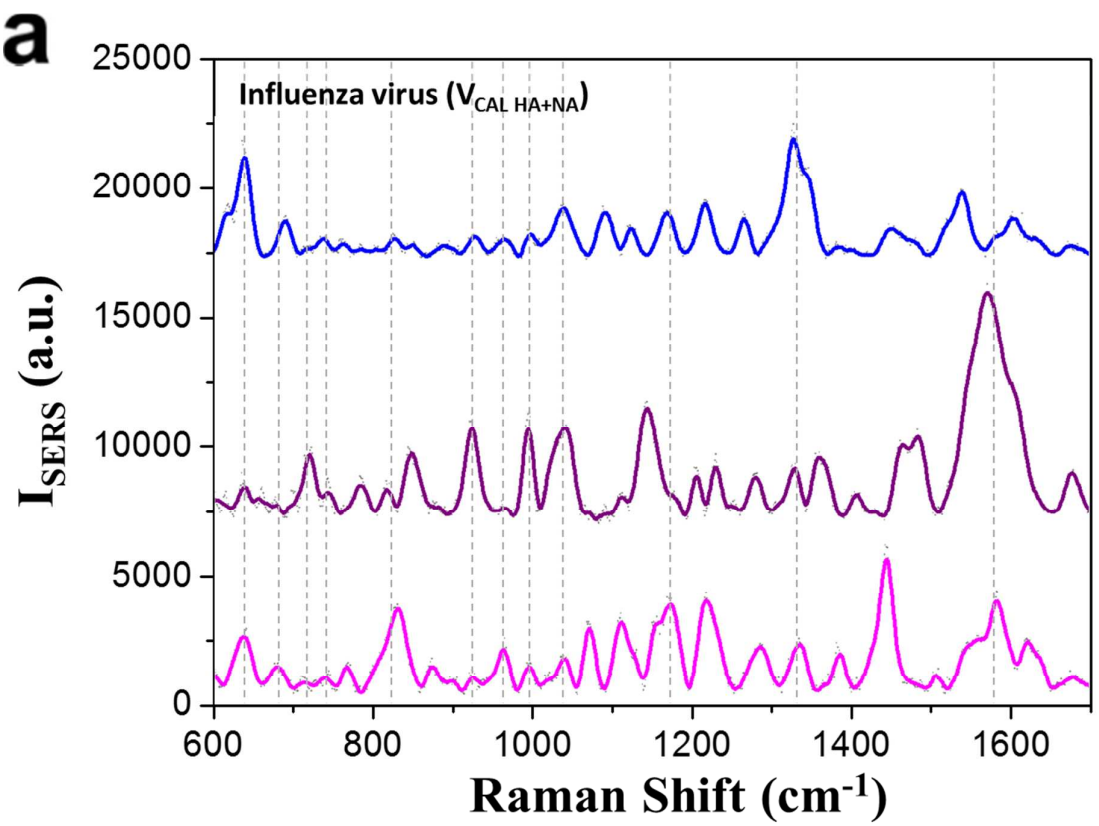
a
Influenza virus ($V_{CAL\ HA+NA}$)
I_{SERS} (a.u.)
25000
20000
15000
10000
5000
0
600
800
1000
1200
1400
1600
Raman Shift (cm^{-1})

Figure S3

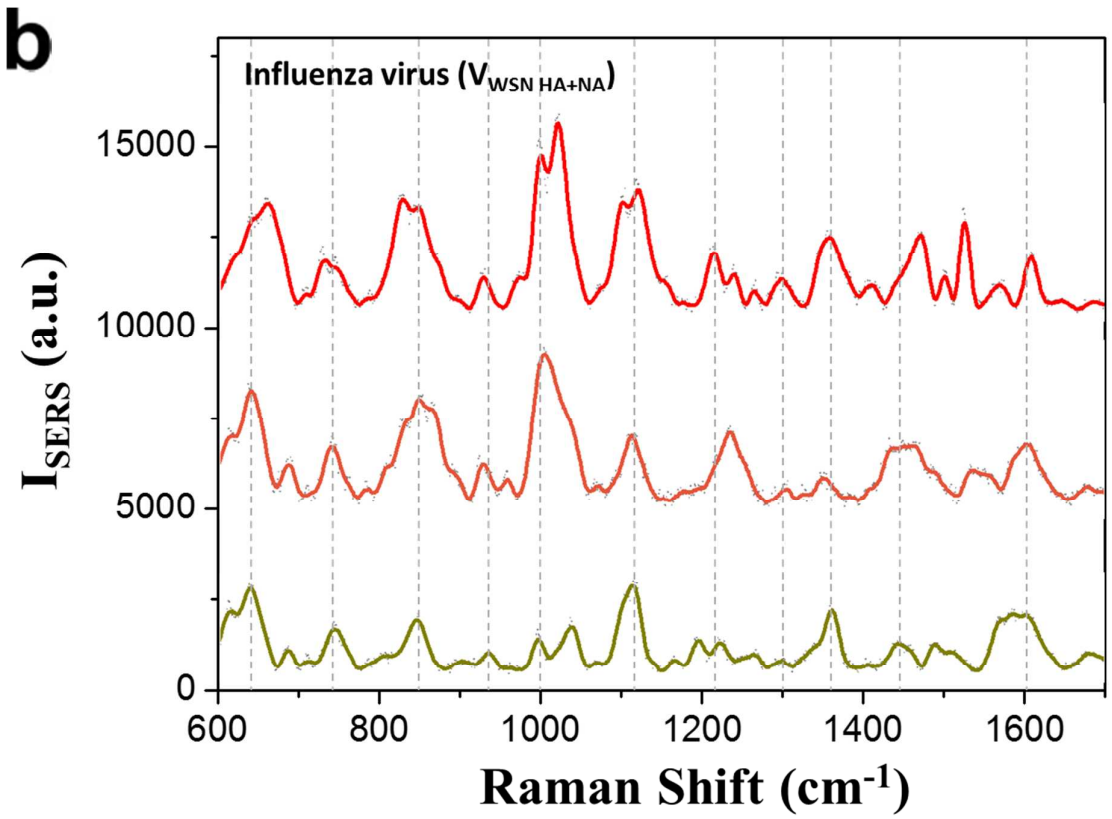

Figure S3. SERS signals of influenza viruses (a) $V_{CAL\ HA+NA}$ (b) $V_{WSN\ HA+NA}$

Since raw Raman signals include random noises and other signals such as the substrate, not only the signal of target molecule, they have been handled by baseline subtraction and noise removal in a majority of researches for Raman detection.[1-4] After postprocessing, Raman spectroscopy is more powerful for molecular sensing, because specific peaks can stand out vividly against the baseline. Postprocessing has generally been used by manual methods or Fourier transform, but we used, here, modified baseline estimation and denoising using sparsity, or BEADS which has been used for chromatography.[5] Simply speaking, it automatically tracks the baseline of raw Raman signal and subtract the baseline from the raw signal, and the high or low pass filter is used for noise canceling. Below is an example of our postprocessing (Figure S4).

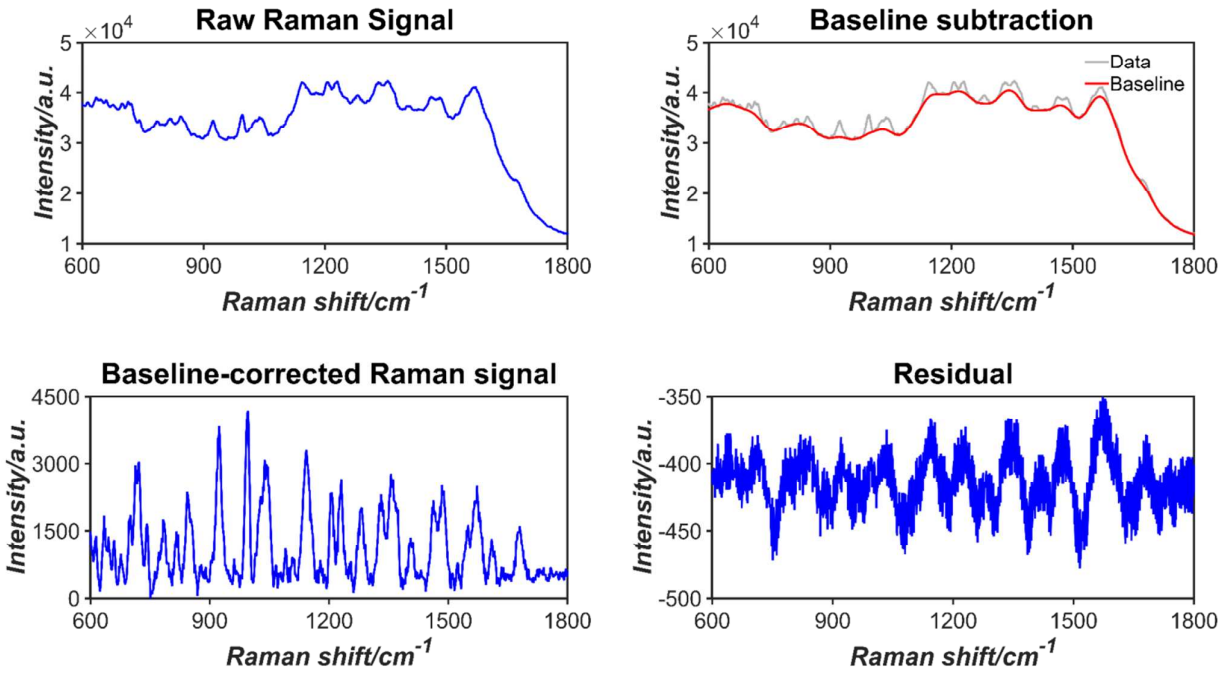

Figure S4. Postprocessing method of SERS signals.

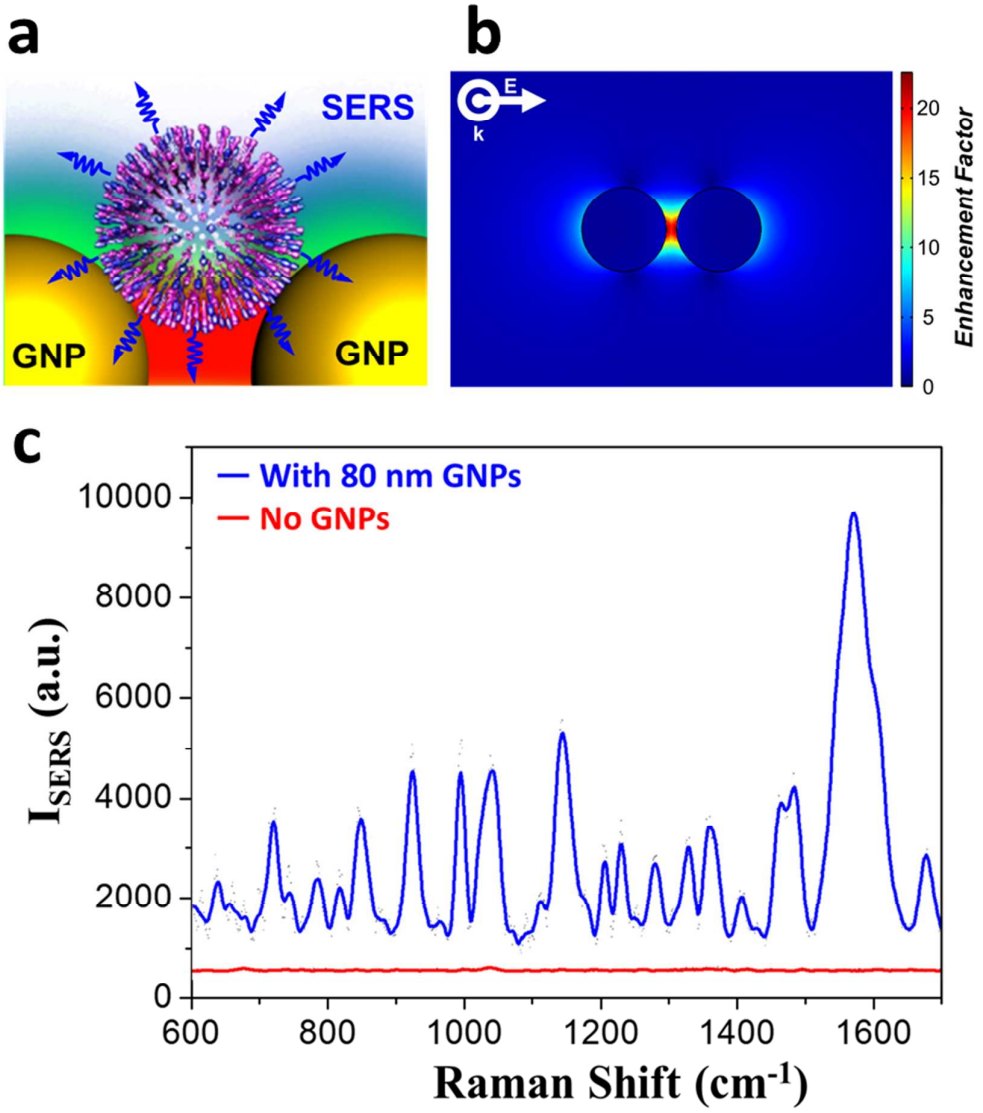

Figure S5. The effect of SERS with GNPs to make "*hot-spot*" *via* SERS.

(a) Schematic diagram of the influenza virus detection *via* SERS. (b) Calculated electric field distribution at the plane parallel to xy plane (z=40 nm). The diameter of GNPs is 80 nm, the gap size between GNPs is 10 nm, and the wavelength of laser is 785 nm. (c) The effect of GNP enhancing Raman scattering. The SERS signal intensity of $V_{CAL\ HA+NA}$ was 2919 fold enhanced at 1573 cm^{-1} by 80 nm GNPs compared with the case without GNPs (thereby the enhancement factor was 2919).

Virus type	Packaging batch	Infectious titer (#/ml)	Genomic titer (#/ml)	The number of genomic particle on the analyzing spot
V_{VSVG}	#1	$2.7 \cdot 10^7$	$1.6 \cdot 10^9$	9.01
	#2	$4.4 \cdot 10^7$	$1.3 \cdot 10^9$	7.50
	#3	$5.5 \cdot 10^7$	$3.0 \cdot 10^9$	16.87
$V_{WSN\ HA+NA}$	#1	$1.5 \cdot 10^6$	$3.3 \cdot 10^9$	18.57
	#2	$2.2 \cdot 10^6$	$1.4 \cdot 10^9$	7.96
	#3	$3.9 \cdot 10^5$	$4.2 \cdot 10^9$	23.60
$V_{CAL\ HA+NA}$	#1	$5.9 \cdot 10^1$	$2.1 \cdot 10^9$	12.06
	#2	$3.6 \cdot 10^1$	$2.9 \cdot 10^9$	16.57
	#3	$5.2 \cdot 10^1$	$4.0 \cdot 10^9$	22.41
$V_{WSN\ HA\ +\ CAL\ NA}$	#1	$9.2 \cdot 10^5$	$1.1 \cdot 10^9$	6.36
	#2	$1.9 \cdot 10^7$	$1.5 \cdot 10^9$	8.45
	#3	$4.1 \cdot 10^6$	$4.0 \cdot 10^9$	22.24
$V_{no\ envelope}$	#1	0.0	N.A.	N.A.
	#2	5.6	N.A.	N.A.
	#3	$1.3 \cdot 10^1$	N.A.	N.A.

Table S1. Genomic and infectious titers of virus samples. Each type of virus was independently packaged and quantified three times. As shown, virus samples packaged in the absence of envelope proteins did not contain a significant level of infectious particles. Based on that the fraction of analyzing spot over the whole nanoparticle substrate area was chosen at 1/2.25E+06 and virus samples were well spread on the substrate, the number of virus genomic particles that likely contributed to generating SERS signals was also theoretically calculated and shown in the last column.

Viruses	600 – 1700 peak (Raman shift) (cm^{-1})																	
V_{VSVG}		638		846		945	994		1067		1124	1172	1231	1264			1564	1587
$V_{CAL\ HA+NA}$	616	638		846	923		994						1231		1356	1463	1564	1587
$V_{WSN\ HA+NA}$	616	638	740	846			994	1015		1107			1231			1463	1564	1587
$V_{WSN\ HA+CAL\ NA}$	616	638	740	846	923		994	1015	1067	1107	1124	1172	1231		1356	1463	1564	1587
PBS	616	638		846			994	1015	1067		1124	1172		1264		1463		1587

Table S2. Summary of the Raman peaks for each virus.